Journal of Statistical Mechanics: Theory and Experiment
An IOP and SISSA journal

Special Issue on Unsolved Problems of Noise in Physics, Biology and Technology

# Spectral density of velocity fluctuations under switching field conditions in graphene

**J M Iglesias, M J Martín, E Pascual and R Rengel**

Department of Applied Physics, University of Salamanca, Salamanca 37008, Spain
E-mail: josem88@usal.es

Received 16 September 2015
Accepted for publication 18 November 2015
Published 20 May 2016

Online at stacks.iop.org/JSTAT/2016/054018
doi:10.1088/1742-5468/2016/05/054018

**Abstract.** In this paper we present an analysis of the velocity fluctuations during transient regimes arising from an abrupt shift of the electric field in bulk monolayer graphene. For this purpose a material Ensemble Monte Carlo simulator is used to examine these fluctuations by means of the transient autocorrelation function and power spectral density. The evolution of these quantities as well as the non-stationary phenomena taking place during the transients is explained with a microscopic approach.

**Keywords:** classical Monte Carlo simulations, fluctuations (theory), transport properties (theory), current fluctuations

J. Stat. Mech. (2016) 054018


1742-5468/16/054018+8$33.00

## Contents



## 1. Introduction

Due to its remarkable properties graphene has become in recent years one of the most fashionable materials for a lot of electronics and optoelectronics applications [1–3]. The unusual gapless linear dispersion relation in the vicinities of the Dirac points is of tremendous interest for being the origin of the massless behaviour that electrons exhibit in this material. The most direct implication of this feature is that electrons in graphene travel at a constant velocity named the Fermi velocity, $v_F \approx 10^8$ cm s$^{-1}$ [4], and therefore carrier velocity along a certain direction depends only on its wavevector orientation. As a result, the velocity fluctuations in graphene are limited [5] to a maximum value of 2 $v_F$ and velocity relaxation through scattering mechanisms depends only on the momentum reorientation, which is strongly affected by the anisotropy of the scattering mechanisms.

As a result of the above-mentioned interest in this material, several studies regarding the investigation of graphene devices have been carried out [6–9]. With the purpose of offering a microscopic study of the inherent sources of noise in the material, we present an analysis of instantaneous velocity fluctuations in graphene by means of computational simulation performed with the Ensemble Monte Carlo Method [10]. The scattering sources taken into account in our simulations are the optical, intravalley and intervalley acoustic phonons, impurities [11] and lattice defects [12]. Short range carrier–carrier interactions are also considered as they have been demonstrated to be a crucial mechanism that degrades both the mobility [13] and the saturation velocity [14].

In most analogue and digital transistor applications, the carriers inside the conducting channel are the subject of changes in applied field conditions. This work focuses on the transient regimes arising from abrupt changes of the magnitude of the applied electric field: from low to high values, and vice versa. The study of the velocity fluctuations in these situations by means of the transient autocorrelation function is defined as [15]

$$C_{\delta v}(t,\tau) = \langle \delta v(t)\delta v(t-\tau)\rangle, \tag{1}$$

where $t$ and $t-\tau$ are the instants for which the correlation is calculated, the angular brackets mean ensemble averages, $\delta v(t) = v(t) - \langle v(t)\rangle$ is the particle velocity



J. Stat. Mech. (2016) 054018

fluctuation, $v(t)$ being the velocity in a specific direction of the particle at instant $t$. The different contributions to the velocity fluctuations are considered [16]:

$$\delta v(t) = \delta v_\varepsilon(t) + \delta v_{\mathbf{k}}(t), \tag{2}$$

where the first term of the right-hand side of the equation is the so-called convective contribution associated with the fluctuations of the electron energy, being $\delta v_\varepsilon(t) = v_\varepsilon(t) - \langle v(t)\rangle$, and $v_\varepsilon(t)$ the average velocity of the particles with an energy between $\varepsilon$ and $\varepsilon + \Delta\varepsilon$ at an instant $t$. The second term is the thermal contribution, $\delta v_{\mathbf{k}}(t) = v(t) - v_\varepsilon(t)$, associated with the fluctuations of the electron momentum orientation. In our graphene model the intervalley term is not considered, as both $K$ and $K'$ valleys are equivalent in terms of electronic transport, i.e. valley drift velocity. So, the autocorrelation function matrix becomes:

$$\begin{aligned}\mathbf{C}_{\delta v}(t,\tau) &= \begin{bmatrix} C_{\delta v,\varepsilon\varepsilon}(t,\tau) & C_{\delta v,\varepsilon\mathbf{k}}(t,\tau) \\ C_{\delta v,\mathbf{k}\varepsilon}(t,\tau) & C_{\delta v,\mathbf{kk}}(t,\tau) \end{bmatrix} \\ &= \begin{bmatrix} \langle \delta v_\varepsilon(t)\delta v_\varepsilon(t-\tau)\rangle & \langle \delta v_\varepsilon(t)\delta v_{\mathbf{k}}(t-\tau)\rangle \\ \langle \delta v_{\mathbf{k}}(t)\delta v_\varepsilon(t-\tau)\rangle & \langle \delta v_{\mathbf{k}}(t)\delta v_{\mathbf{k}}(t-\tau)\rangle \end{bmatrix},\end{aligned} \tag{3}$$

$C_{\delta v,\varepsilon\varepsilon}$ and $C_{\delta v,\mathbf{kk}}$ being the convective and thermal terms, respectively. The analysis is completed with the transient power spectral density (TPSD), described as [17]

$$S_{\delta v}(t,f) = \frac{1}{t-t_0}\left\langle \left| \int_{t_0}^{t} \delta v(\tau) \mathrm{e}^{2\pi \mathrm{i} f(\tau - t_0)} \mathrm{d}\tau \right|^2 \right\rangle, \tag{4}$$

with $t_0$ being the instant of the electric field switch. For most practical applications, graphene is used lying on top of a substrate. Therefore, besides suspended graphene the velocity fluctuations of graphene on two different substrates ($SiO_2$ and h-BN) are also analysed. In the case of graphene on a substrate, the influence of the latter is considered by the inclusion of the surface polar phonon (SPP) modes [18, 19] that couple to the electrons in the graphene layer, and the additional screening provided by means of the background dielectric constant, $\bar{\kappa} = (1 + \kappa^0_{\mathrm{sub}})/2$, where $\kappa^0_{\mathrm{sub}}$ is the substrate low-frequency dielectric constant.

## 2. Results

First, we adjust the impurity density and the defect parameters in our simulator, so that the mobility for graphene on $SiO_2$ as a function of the carrier density reproduces the experimental results in [20]. The values considered for the impurity density and the defect parameter [12] are $n_{\mathrm{imp}} = 0.95 \times 10^{12}$ cm$^{-2}$ and $\alpha_{\mathrm{def}} = 0.07$ eV nm respectively, and will be unchanged for suspended graphene and graphene on h-BN for comparison purposes.

According to this fit, figure 1(a) shows the velocity-field curves for suspended graphene, graphene on h-BN and on $SiO_2$ substrates. It is remarkable that the parallel velocities of graphene on $SiO_2$ and h-BN substrates are noticeably larger than for suspended graphene. This is mainly due to the effect of the scattering with SPPs. This interaction reduces the carrier energy, but produces only a slight momentum reorientation

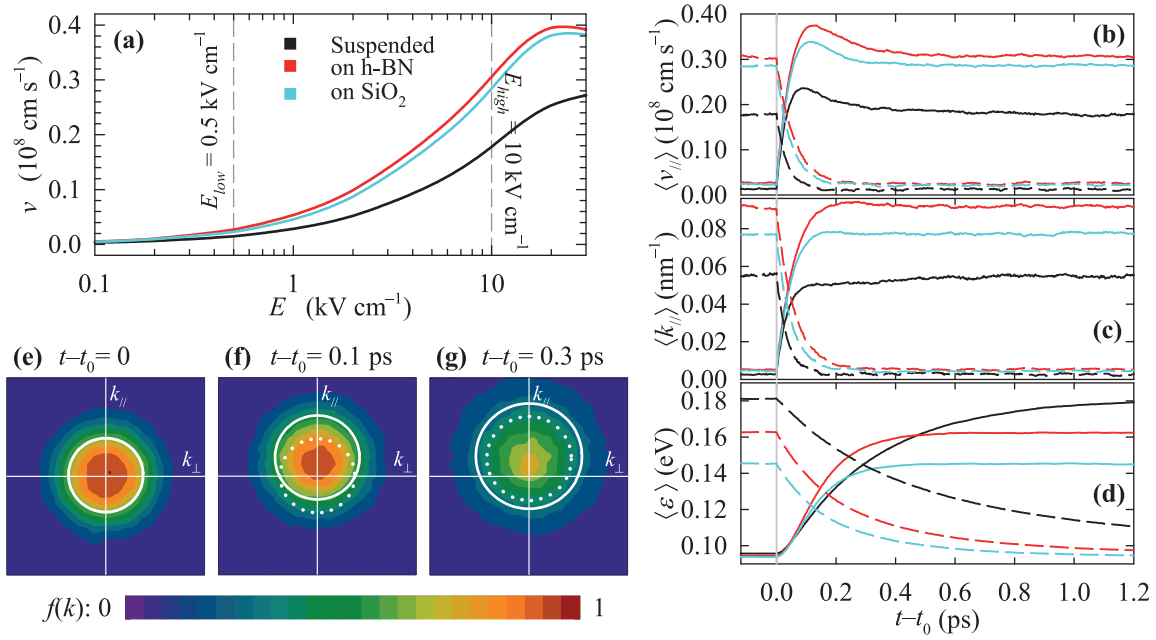


**Figure 1.** (a) Parallel velocity as a function of the applied electric field for suspended monolayer graphene, graphene on h-BN and on $SiO_2$. The high and low electric fields that define the switching conditions are shown as vertical dashed lines. Average quantities: (b) parallel velocity, (c) parallel wavevector and (d) energy as a function of time for the transients from low-to-high field (solid lines) and from high-to-low field (dashed lines) for the three cases under study. $t_0$ is the instant at which the electric field is switched. Distribution functions in momentum space for the low-to-high field transient at different intervals $t - t_0$: (e) 0 (low field stationary state), (f) 0.1 ps and (g) 0.3 ps of graphene on $SiO_2$. The white solid circles represent the average thermal energy centered at the average wavevector for the given situation, while the dotted ones show for comparison the circles of the previous situation.

due to its Coulombic nature [19]. We choose a low field $E_{\text{low}}$ such that the average drift velocity in the direction of the applied field is low but still noticeable, and a high field $E_{\text{high}}$ for which the ensemble velocity is around ten times larger than that for the low field. Figures 1(b)–(d) depict, as a function of time, the transient velocity in the direction of the applied field, the momentum and the energy averaged over the ensemble. In the low-to-high field transient the three cases under study undergo a velocity overshoot before reaching the stationary value, while the parallel wavevector reaches its maximum at around 0.2 ps and stays steady thereafter. The average energy presents a slower evolution and marks out the time lapse of the transients, which is 0.6 ps for graphene on substrates and over 1.2 ps for suspended graphene. This transient is dominated by an initial strong drag of the high electric field that pushes the carrier distribution against its direction in momentum space (figure 1(e)). Afterwards, the distribution increases its electronic temperature, i.e. it tends to spread, but remaining displaced from the Dirac point, resulting in a steady value of the averaged momentum but a reduction of the ensemble velocity and rise of the energy (figure 1(g)). With regard to the high-to-low field transient, the parallel velocity and wavevector evolve with a similar

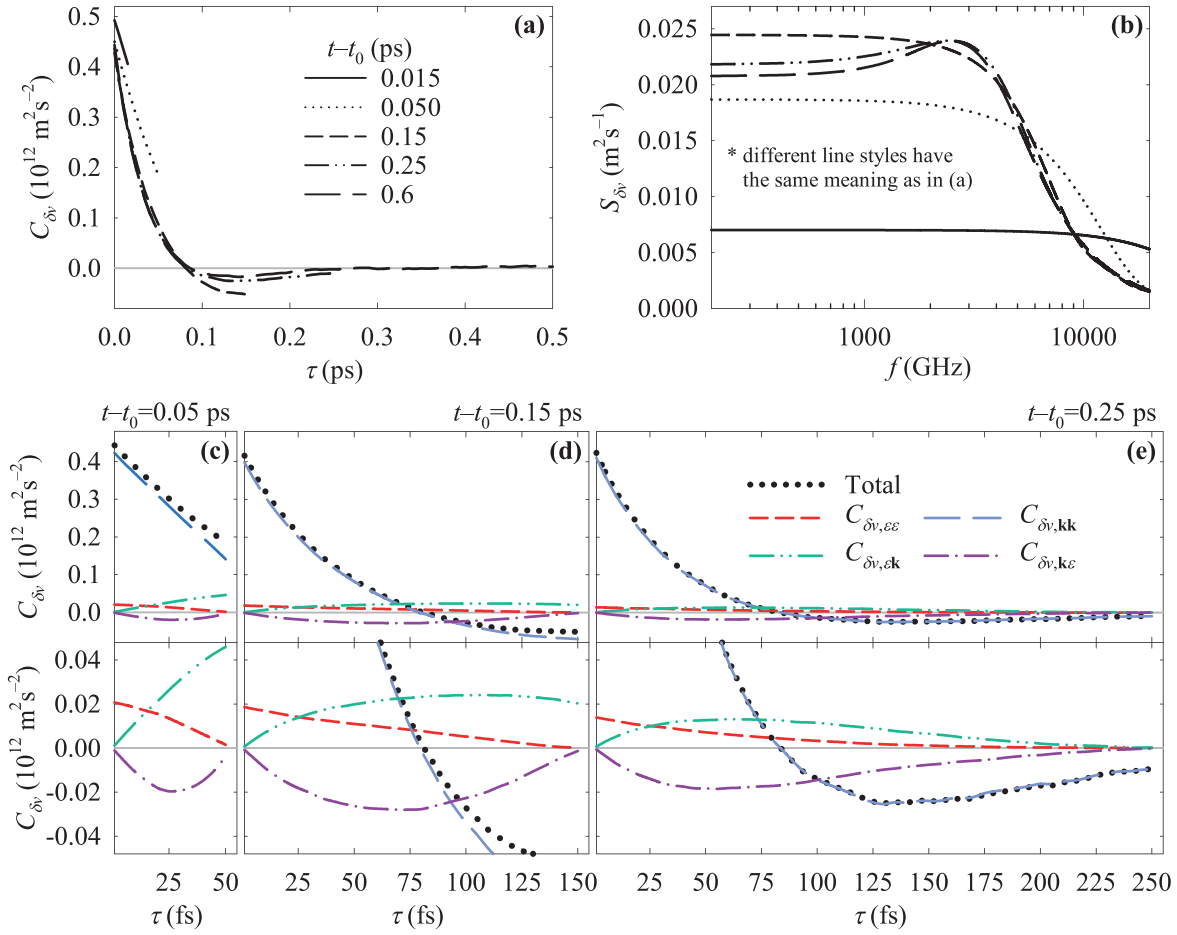


**Figure 2.** Low-to-high field transient (a) autocorrelation function and (b) transient power spectral density of the velocity fluctuations for graphene on $SiO_2$ at different instants. The considered components of the autocorrelation function at $t - t_0$: (c) 0.05 ps, (d) 0.15 ps and (e) 0.25 ps, arising from the contributions of the velocity fluctuations, as shown in equations (2) and (3).

trend, arriving at a stationary value at 0.2 ps while the energy decay is slower, again the suspended graphene presenting the longest transient time. Here, the dynamics of the ensemble happens in a similar way. First, the hot momentum displaced distribution, gets closer to the Dirac point in the absence of a high electric field, and then it cools down. In contrast to the previous case, this transient is only ruled by the effect of the scattering mechanisms that lead the system to a stationary state closer to the equilibrium.

Let us now focus on the graphene on the $SiO_2$ configuration. In figure 2(a) we plot the transient autocorrelation function for various instants after the applied low-to-high step in the electric field. At the earliest times the initial value of the autocorrelation decreases as the ensemble velocity grows. Also, a progressive steepening of the initial slope and a minimum at around 0.14 ps can be seen. Both phenomena are a consequence of the increasing scattering activity that takes place as the electric field makes the carrier distribution more energetic and shifted in momentum space. In this situation, hot carriers would mostly move with a higher velocity than the ensemble average (positive velocity fluctuation) and are due to be backscattered with optical or intervalley

J. Stat. Mech. (2016) 054018

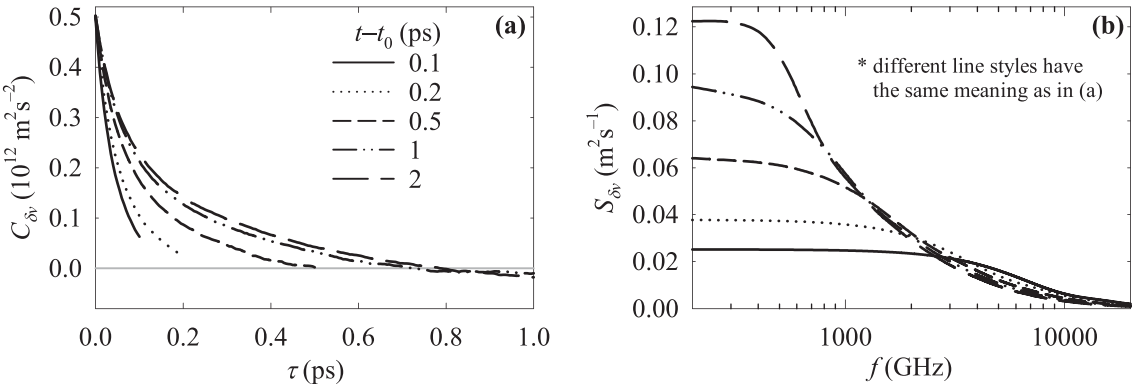


**Figure 3.** High-to-low field transient (a) autocorrelation function and (b) transient power spectral density of the velocity fluctuations for graphene on $SiO_2$ at different instants.

acoustic phonons with a resulting velocity lower than the ensemble average, and therefore acquire a negative velocity fluctuation. On the other hand, cold carriers would have a velocity lower than the ensemble average (negative velocity fluctuation) and because of the drag of the electric field, they get hotter and reach a positive (or at least closer to zero) velocity fluctuation before undergoing the same process described above. This results in a change of the sign of the velocity fluctuations, causing the increasingly faster decay and the negative part of the autocorrelation function. For longer times ($t - t_0 = 0.6$ ps), the value of the minimum moderates itself, and the autocorrelation function mostly approaches that of the stationary situation for $E = E_{\text{high}} = 10$ kV cm$^{-1}$. The results indicate (figures 2(c)–(e)) that the dominant contribution is the thermal one, corresponding to the momentum fluctuations. However, for this transient, the convective contribution (related to the energy fluctuation), although relatively low, is not negligible. This convective term appears as a direct consequence of an initial temporary appearance of a positive fluctuation of newly occupied energy levels, happening concurrently with the velocity overshoot. In figure 2(b) the transient power spectral density (TPSD) provides information about the velocity fluctuation phenomena in the frequency domain. The TPSD grows to achieve the Lorentzian-like shape up to 0.15 ps, and from that moment a maximum starts to appear at 2.5 THz and the low-frequency values start to drop. The frequency of this maximum progressively shifts towards lower energies and the values of the spectral density decrease until reaching the stationary behaviour corresponding to the final electric field.

Figures 3(a) and (b) allow an examination of the velocity fluctuations for the high-to-low field transient in the same procedure as in the previous case. Here, the autocorrelation function evolves by reducing its slope as time passes, which indicates that the velocity fluctuations change their sign less frequently as the transient evolves. Microscopically, this can be explained in terms of the almost non-existence of the available states associated with large negative velocity fluctuations, since the distribution function is very close to the Dirac point. A minimum is achieved at long times (around 1.5 ps), standing out the reduced scattering activity relocating the particle velocity in this transient. In this case, the convective term can be totally disregarded, meaning that there is no noticeable change in the averaged carrier velocities in the different

J. Stat. Mech. (2016) 054018

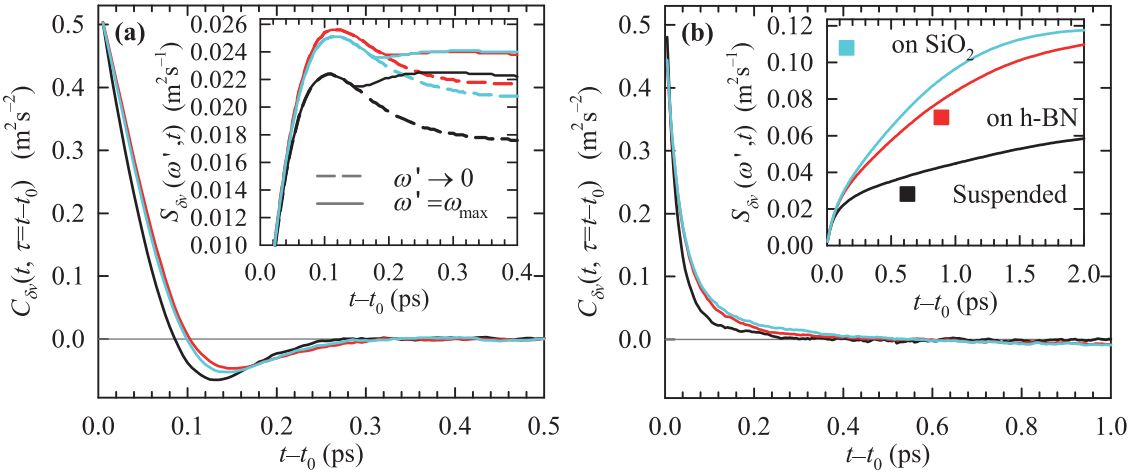


**Figure 4.** Temporal evolution of the correlation of the velocity fluctuations between times $t$ and $t_0$ ($\tau = t - t_0$) and (insets) the power spectral densities at low and maximum frequencies in the (a) low-to-high and (b) high-to-low field transients.

energy levels, and only the wavevector reorientation plays a role in this transient. Finally, the power spectral density reveals that the power dissipated due to velocity fluctuations is larger at low frequencies with a progressively decreasing range with time.

Finally, a brief comparative analysis between the three cases (suspended graphene, graphene on $SiO_2$ and graphene on h-BN) is provided. The suspended graphene showed the fastest response to the electric field shift with regard to the parallel velocity and momentum, but the slowest for the average carrier energy (figures 1(b)–(d)). In the graphene on h-BN and $SiO_2$ the trends are very similar, as the only differences are the substrate polar phonons energies and the background permittivity, while in suspended graphene this interaction with remote polar phonons does not exist and the smaller screening enhances the interaction with impurities. Figure 4(a) shows the evolution of the autocorrelation of velocity fluctuations at time $t$ and the initial conditions ($\tau = t - t_0$). In the low-to-high transient, the velocity fluctuations correlation is lost at shorter times in suspended graphene, followed by graphene on $SiO_2$ and on h-BN, and the minimum is reached at 0.125 ps, while for graphene on $SiO_2$ and h-BN it is at 0.140 and 0.150 ps, respectively. Also, the shorter the time at which the minimum is reached, the lower its value. In figure 4(b) the evolution of the TPSD at low frequencies (dotted line) and its maximum value (solid line) is shown. Both curves coincide until the appearance of the maximum in the power spectral density, which is located at frequencies of 2.2 THz for graphene on h-BN and 2.6 THz for suspended graphene, and whose value remains almost steady for graphene on the substrates, but varies in time for the suspended layer. The low-frequency power spectral density evolution shows similar trends for the three cases: a fast initial rise until reaching a maximum, followed by a smooth drop and its stabilisation towards the value of the high field stationary. With regard to the high-to-low field transient, although the initial correlation is higher for suspended graphene, it presents a faster decay of the velocity correlation. As it concerns the low-frequency power spectral density, for the three cases it grows until saturation for times longer than 2.0 ps.

J. Stat. Mech. (2016) 054018

## 3. Conclusions

Velocity fluctuations under transient field conditions in monolayer graphene were studied by means of an ensemble material Monte Carlo simulator. In the low-to-high field transient the quick response of the electrons to the high field results in a velocity overshoot. The transient velocity fluctuation correlation function tends to decrease over time, and reaches a minimum between 120 and 140 fs, which corresponds to a maximum value of the power dissipated by the velocity fluctuations around 2.3 THz. Finally, for the high-to-low field transient, the velocity fluctuation correlation function increases over time because of the progressive lessening of the velocity reorientation by the scattering mechanisms. In comparison, velocity fluctuations in graphene on substrates show similar behaviour. However, when considering a suspended layer, a faster loss of the autocorrelation and lower values on the power spectral density are achieved as a consequence of the absence of substrate interactions. Clearly, the dominant term contributing to the velocity fluctuations is the thermal one; nevertheless, in the low-to-high transient the convective contribution is noticeable due to the fast shift of the electron distribution in the momentum space as a response to the change towards a higher electric field.

## Acknowledgments

This work was supported by research project TEC2013-42622-R from the *Ministerio de Economía y Competitividad*.

## References

[1] Avouris P 2010 *Nano Lett.* **10** 4285–94
[2] Zheng J, Wang L, Quhe R, Liu Q, Li H, Yu D, Mei W N, Shi J, Gao Z and Lu J 2013 *Sci. Rep.* **3** 1314
[3] Liu C H, Chang Y C, Norris T B and Zhong Z 2014 *Nat. Nanotechnol.* **9** 273–8
[4] Neto A H C, Guinea F, Peres N M R, Novoselov K S and Geim A K 2009 *Rev. Mod. Phys.* **81** 109–62
[5] Rengel R and Martín M J 2013 *J. Appl. Phys.* **114** 143702
[6] Rumyantsev S, Liu G, Stillman W, Shur M and Balandin A A 2010 *J. Phys.: Condens. Matter* **22** 395302
[7] Moon J S *et al* 2011 *IEEE Electron Device Lett.* **32** 270–2
[8] Pal A N, Ghatak S, Kochat V, Sneha E S, Sampathkumar A, Raghavan S and Ghosh A 2011 *ACS Nano* **5** 2075–81
[9] Zhang Y, Mendez E E and Du X 2011 *ACS Nano* **5** 8124–30
[10] Sze S M 1981 *Phys. Semicond. Devices* (New York: Wiley-Interscience)
[11] Adam S, Hwang E, Rossi E and Sarma S D 2009 *Solid State Commun.* **149** 1072–9
[12] Ferry D K 2013 *J. Comput. Electron.* **12** 76–84
[13] Li X, Barry E A, Zavada J M, Nardelli M B and Kim K W 2010 *Appl. Phys. Lett.* **97** 082101
[14] Fang T, Konar A, Xing H and Jena D 2011 *Phys. Rev.* B **84** 125450
[15] Brunetti R and Jacoboni C 1984 *Phys. Rev.* B **29** 5739–48
[16] Brunetti R and Jacoboni C 1983 *Phys. Rev. Lett.* **50** 1164–67
[17] Sánchez T G, Pérez J E V, Conde P M G and Collantes D P 1992 *Appl. Phys. Lett.* **60** 613
[18] Perebeinos V and Avouris P 2010 *Phys. Rev.* B **81** 195442
[19] Rengel R, Pascual E and Martín M J 2014 *Appl. Phys. Lett.* **104** 233107
[20] Dorgan V E, Bae M H and Pop E 2010 *Appl. Phys. Lett.* **97** 082112



J. Stat. Mech. (2016) 054018